Cancer Therapy: Clinical

Clinical Cancer Research

The Relationship Between Homologous Recombination Repair and the Sensitivity of Human Epidermis to the Size of Daily Doses Over a 5-Week Course of Breast Radiotherapy

Navita Somaiah[1,2], John Yarnold[2], Frances Daley[2], Ann Pearson[2], Lone Gothard[2], Kai Rothkamm[3], and Thomas Helleday[4]

Abstract

Purpose: A molecular understanding of tissue sensitivity to radiotherapy fraction size is missing. Here, we test the hypothesis that sensitivity to fraction size is influenced by the DNA repair system activated in response to DNA double-strand breaks (DSB). Human epidermis was used as a model in which proliferation and DNA repair were correlated over 5 weeks of radiotherapy.

Experimental design: Radiotherapy (25 fractions of 2 Gy) was prescribed to the breast in 30 women with early breast cancer. Breast skin biopsies were collected 2 hours after the 1st and 25th fractions. Samples of contralateral breast skin served as controls. Sections were coimmunostained for Ki67, cyclin A, p21, RAD51, 53BP1, and β1-integrin.

Results: After 5 weeks of radiotherapy, the mean basal Ki67 density increased from 5.72 to 15.46 cells per millimeter of basement membrane ($P = 0.002$), of which the majority were in S/G2 phase, as judged by cyclin A staining ($P < 0.0003$). The p21 index rose from 2.8% to 87.4% ($P < 0.0001$) after 25 fractions, indicating cell cycle arrest. By week 5, there was a 4-fold increase ($P = 0.0003$) in the proportion of Ki67-positive cells showing RAD51 foci, suggesting increasing activation of homologous recombination.

Conclusions: Cell cycle arrest in S/G2 phase in the basal epidermis after a 5-week course of radiotherapy is associated with greater use of homologous recombination for repairing DSB. The high fidelity of homologous recombination, which is independent of DNA damage levels, may explain the low-fractionation sensitivity of tissues with high-proliferative indices, including self-renewing normal tissues and many cancers. *Clin Cancer Res; 18(19); 5479–88. ©2012 AACR.*

Introduction

Clinical radiotherapy is delivered as a sequence of fractional, usually daily, doses. Tissues vary in their sensitivity to several treatment-related variables, including total dose, fraction size, interfraction interval, and overall treatment time (1). On average, cancers are less sensitive to fraction size than the normal tissues responsible for most dose-limiting complications months or years later (2). High total doses (>60 Gy) delivered in small (2.0 Gy) fractions spare normal tissues relative to most malignancies, and achieve the highest level of tumor control for a given level of chronic adverse effects. Recent level 1 evidence indicates that breast and prostate cancer are more sensitive to fraction size than commonly assumed (3–5). An understanding of molecular mechanisms is, therefore, needed to ensure effective selection of fractionation schedule in individual patients.

Fraction size sensitivity is a cellular property reflecting, the ability to repair otherwise lethal DNA double-strand breaks (DSB) before the next fraction of radiotherapy (6). DSB are rapidly repaired by nonhomologous end-joining (NHEJ) in all phases of the cell cycle, in addition to which, homologous recombination requiring an intact sister chromatid, repairs a proportion of DSB in S and G2 phases of the cell cycle (7–9). Fractionation sensitivity is associated with the proliferative status of a tissue, being higher in tissues with low-proliferative indices, and vice versa (10). Rodent cell lines deficient in NHEJ are very radiation sensitive, relying disproportionately on homologous recombination to repair DSB and showing no dose-rate sparing, an indicator of insensitivity to fraction size (11). We postulated that the high fidelity of DSB repair in replicated chromatin (12, 13), which is independent of DNA damage levels, may

Authors' Affiliations: [1]Gray Institute for Radiation Oncology & Biology, University of Oxford, Oxford, UK; [2]The Royal Marsden NHS Foundation Trust & Institute of Cancer Research, Sutton, Surrey, UK; [3]Health Protection Agency, Centre for Radiation, Chemical & Environmental Hazards, Chilton, Didcot, Oxon, UK; and [4]Science for Life Laboratory, Division of Translational Medicine and Chemical Biology, Department of Medical Biochemistry and Biophysics, Karolinska Institutet, Stockholm, Sweden

Note: Supplementary data for this article are available at Clinical Cancer Research Online (http://clincancerres.aacrjournals.org/).

Corresponding Authors: Thomas Helleday, Science for Life Laboratory, Karolinska Institutet, BOX 1031, S-171 21 Stockholm, Sweden. Phone: 46-0852480000; Fax: 2086613107; E-mail: thomas.helleday@scilifelab.se; Kai Rothkamm, E-mail: kai.rothkamm@hpa.org.uk; and John Yarnold, E-mail: John.yarnold@icr.ac.uk

doi: 10.1158/1078-0432.CCR-10-3297

Translational Relevance

The dose of curative radiotherapy for cancer is commonly limited by normal tissue damage causing complications years later. These tissues are, on average, more sensitive to the size of daily doses (fractions) than cancers and have lower proliferative indices. Small (2 Gy) fractions therefore spare normal tissues relative to cancer with increased tumor control for a given level of complications. An understanding of the molecular basis of fraction size sensitivity is necessary to improve radiotherapy outcome. Sensitivity to fraction size is inversely correlated to the proliferative indices of normal tissues and, probably, of cancers too. Using human epidermis as a model, we show that homologous recombination repair of radiation-induced DNA double-strand breaks is progressively activated during a course of radiotherapy. This offers a mechanistic explanation for the relative insensitivity to fraction size of normal and malignant tissues characterized by high-proliferative indices, and suggests a potential approach to individualization of dose per fraction.

explain the low-fractionation sensitivity of tissues with high-proliferative indices, including self-renewal normal tissues and many cancers.

The epidermis in patients undergoing radiotherapy for breast cancer offers a readily accessible system for investigating DSB repair in different proliferative states. Early in the course of treatment, clinical data suggest that the epidermis is more sensitive to fraction size than at the end of a 5-week schedule of radiotherapy as showed by Turesson and colleagues in breast cancer patients irradiated with various dose schedules (10, 14). Before radiotherapy, basal epidermal cells are predominantly in nonproliferative phase, but proliferative markers and cell cycle checkpoints change over the course of 5 weeks radiotherapy (15, 16). DSB rejoining can be monitored in tissue sections using antibodies against 53BP1 as a surrogate for DSB and antibodies against RAD51 as a biomarker of homologous recombination (17).

Materials and Methods

Patients and radiotherapy

A total of 30 patients prescribed radiotherapy to a dose of 50 Gy in 25 fractions (2.0 Gy per fraction) over 5 weeks to the breast after tumor excision of early breast cancer were recruited with written informed consent. Radiotherapy was delivered to the whole breast using tangential 6 to 10 MV X-ray beams. We adhered to the International Commision on Radiation Units and Measurements (ICRU) recommendations to keep dose inhomogeneity between 95% and 105% in the target volume and three-dimensional dose compensation was used to achieve homogeneity. The estimated dose to the skin was 1.6 Gy per fraction. Ethical and scientific approval for the study was granted by the Royal Marsden Hospital Research Ethics Committee (REC No: 06/Q0801/73) and Committee for Clinical Research (CCR 2900).

Tissue collection and processing

Single 4 mm punch biopsies of breast skin were collected at the following time points and locations:

(i) 2 hours (h) after the 1st fraction from irradiated and contralateral breast.
(ii) 2 hours after the 5th fraction from irradiated breast.
(iii) 1 hour before and 2 hours after the final (25th) fraction from irradiated breast.

Local anesthetic (0.5–1 mL lidocaine) was infiltrated subcutaneously before biopsies collected at least 2 cm inside the lateral border of the breast volume and at least 1 cm apart. Steri-strips plus dry nonadhesive gauze were applied to approximate the wound edges. Biopsies were fixed in 10% neutral buffered formalin, embedded in paraffin and cut into 4 μm sections. Four punch biopsies, 2 from the irradiated breast and 2 from the unirradiated breast, were collected immediately after the 25th fraction of radiotherapy in 3 patients. One paired sample from each of the 3 patients was snap frozen in liquid nitrogen and the other fixed in formalin. No problems with healing or infection were encountered.

Immunohistochemical technique

To avoid loss of tissue section adherence following antigen retrieval, all sections were picked up onto either superfrost plus or superfrost gold slides and placed on a hot plate at 60°C for 10 minutes before starting. Deparaffinized and rehydrated samples were then microwaved at 850 W in 250 mL of 10 mmol/L citric acid (pH adjusted to 6.0) for 12 minutes (3 × 4 minutes). They were then left to stand at room temperature for 20 minutes, before being washed in running tap water, rinsed in TBS, and the section circled with a resin pen. We conducted double staining in layers as described before (18; for all antibody details please refer to Table 1). Briefly, after treating with DAKO peroxidase and protein block for 5 minutes each, the sections were incubated with β1 integrin (CD29) for 1 hour at room temperature. After washing with TBS, mouse/rabbit Dako EnVision horseradish peroxidase (HRP) was applied for 30 minutes. Following further washing in TBS, diaminobenzadine (DAB) solution was applied for 2 minutes. For the second layer of staining, 250 mL of 10 mmol/L citric acid (pH adjusted to 6.0) was brought to the boil by microwaving at 850 W for 4 minutes and the slides immersed in it for 1 to 2 minutes (to remove any unbound antibody) before cooling down to room temperature. Dako protein block was again applied for 5 minutes, and the sections were incubated for 1 hour at room temperature with Ki67 (MIB-1) or 53BP1 antibody. Similar to the first layer, mouse/rabbit Dako EnVision HRP was applied for 30 minutes followed by Vector SG (Vector laboratories) for 5 to 10 minutes.

Table 1. Antibodies used in the study

Marker	Source	Clone	Species	Cat. no.	Dilution
β1 Integrin	Novocastra	7F10	Mouse	NCL-CD29	1:150–1:300
MCSP	Abcam	LHM2	Mouse	Ab20156	1:400–1:800
Ki67	Novocastra	Polyclonal	Rabbit	NCL-Ki67p	1:1000
Ki67	Dako	MIB-1	Mouse	M7240	1:50
Cyclin A	Novocastra	6E6	Mouse	NCL-CyclinA	1:25–1:50
p21	Novocastra	4D10	Mouse	NCL-L-WAF-1	1:30
RAD51	Abcam	51RAD01	Mouse	Ab1837	1:25
53BP1	Bethyl Labs	Polyclonal	Rabbit	A300-272A	1:100–1:300

Counterstaining was conducted using methyl green (Surgipath) for 20 seconds followed by dehydration, clearing in xylene and mounting in DPX (a standard mounting media in histology containing distyrene, a plasticizer, and xylene).

Cyclin A and p21 single staining was done on serial 4 μm sections of epidermis as described above for the first layer. To compare β1 integrin staining with melanoma chondroitin sulphate proteoglycan (MCSP), which works best on fresh frozen skin samples, we obtained paired biopsies from 3 patients, one of which was fixed in formalin and the other snap frozen. For MCSP staining, the snap frozen skin biopsies were embedded in cryogel, sectioned and fixed in cold acetone for 10 minutes. No antigen retrieval was required. After peroxidase and protein block, the sections were incubated with the MCSP antibody for 60 minutes at room temperature followed by EnVision HRP and DAB as described above. Haematoxylin was used as the counterstain.

Immunofluorescence technique

For double fluorescent staining, the sections were deparaffinized, rehydrated, and heat-mediated antigen retrieval carried out as above. After 5 minutes in Dako protein block, the sections were incubated with RAD51 (51RAD01) and Ki67 (NCL-Ki67p) antibody for 60 minutes at room temperature. After washing with 3% fetal calf serum (FCS) in PBS, Alexa Fluor 488-conjugated goat anti-mouse immunoglobulin G (IgG; Invitrogen, 1:200) and TRITC-conjugated donkey anti-rabbit IgG (1:200) was applied for 60 minutes in the dark at room temperature. This was followed by washing with 3% FCS and staining with 4′, 6-diamidino-2-phenylindole (DAPI; 1:200) for 5 minutes. The slides were air dried and mounted in Vectashield. Double staining with 53BP1 and Ki67 (MIB-1) as well as Ki67 (NCL-Ki67p) and cyclin A was done in a similar fashion. Secondary antibody combinations (conjugated with Alexa Fluor 488 or 555, all at 1:200 dilutions) were applied as appropriate.

Analysis of immunohistochemistry

The entire interfollicular basal compartment was analyzed in each section. Analysis of the immunohistochemical data was undertaken by visual inspection and counting of the slides at high power (X60) and was facilitated for some of the analyses by capturing digital images using an Axioscope trans-illumination microscope (Zeiss) connected to a 3 charged-coupled devices (CCD) color camera (JVC) connected to a PC with a Matrox Meteor frame grabber in a peripheral component interconnect (PCI) bus. The basement membrane length was measured using a calibrated line tool developed in Visilog 5.02 software (Noesis Vision Inc.). β1 integrin and p21 staining was scored as negative (−), weak (+), moderate (++), or strong (+++) depending on intensity of staining. Only cells that were attached to the basement membrane and had moderate to strong uptake of β1 integrin along the entire cell membrane were considered to be positive (putative stem cells). Any nuclear uptake of Ki67 (positive in all phases of cell cycle except G0) or cyclin A (S-G2 phase marker) was scored as positive.

Analysis of immunofluorescence

All analysis was done manually at 100× in oil using a Nikon Eclipse TE200 epifluorescence microscope. Digital images were obtained with a cooled analog camera via a video frame grabber and PC. To study the DNA DSB repair pathways in the proliferating versus nonproliferating cell population of the basal epidermis, we looked at RAD51 and 53BP1 foci numbers in all Ki67 positive versus negative cells along the basement membrane. To assess what proportion of proliferating cells were in S-G2 phase of the cell cycle, all $Ki67^+$ cells in the section were analyzed for cyclin A uptake by costaining.

Statistical analysis

Paired Student *t* test (2-tailed) was applied to compare the results from the different time points. The level of significance was taken as $P < 0.05$. One star refers to a P value of <0.05, two stars $P < 0.01$, and three stars $P < 0.001$.

Results

Patient characteristics

The mean age of patients recruited was 58 years. Three patients experienced grade 3 erythema and 3 had moist desquamation in the inframammary fold toward the end of radiotherapy. None of the patients recorded severe late toxicities after 5 years of follow-up. To our knowledge, none of these patients had BRCA1/2-associated familial cancers.

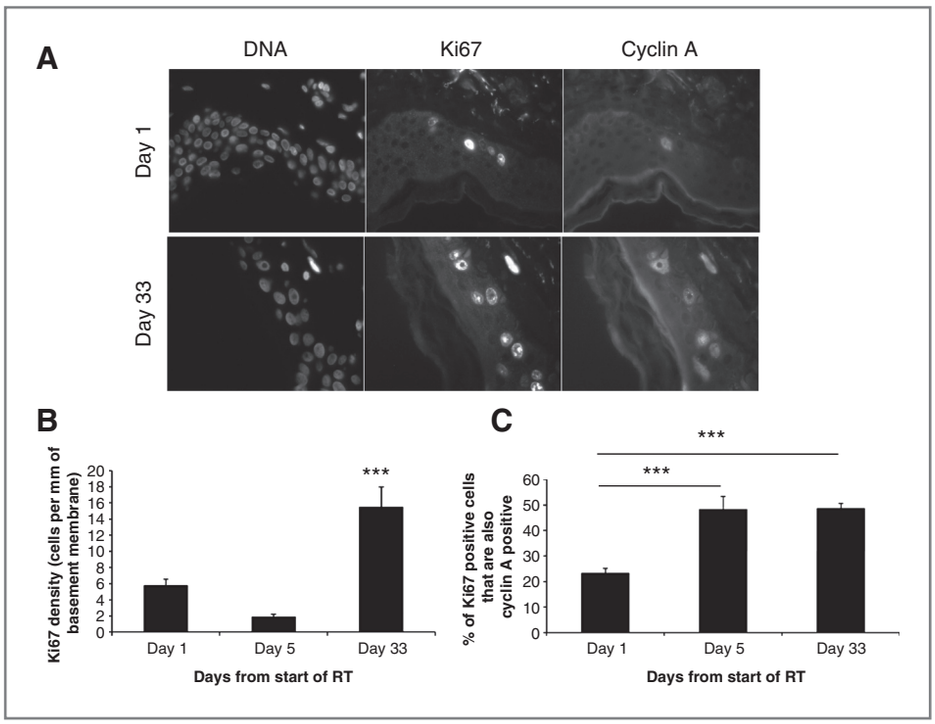

Figure 1. Changes in Ki67 expression in human epidermis during radiotherapy. A, double immunofluorescent staining of human epidermis with Ki67 (panel 2), cyclin A (panel 3), and DAPI counterstain (panel 1) at the beginning and end of radiotherapy (100×). B, the variation of mean basal Ki67 density during the course of radiotherapy. C, the percentage of cycling cells (Ki67 positive) that were in S-G2 phase of the cell cycle (cyclin A positive) increased significantly by week 1 of radiotherapy (48%) and this increase was maintained at the end of 5 weeks (49%, $P < 0.0003$). Error bars show *SEM* in 15 patients. RT, radiotherapy.

Accumulation of cells expressing Ki67, cyclin A, and p21 by the end of 5 weeks radiotherapy

A majority of basal cells showed changes in Ki67 tissue immunohistochemistry (IHC) during the course of radiotherapy (Fig. 1A). The mean basal Ki67 density (cells per mm of basement membrane) increased from 5.72 to 15.46 per mm of basement membrane by the end of the week 5 ($P = 0.002$; Fig. 1B). Immunostaining for cyclin A protein identified the proportion of cells in the late S and G2 phases of the cell cycle. Basal cyclin A index (number of positive cells/total number of cells in basal layer) rose from 3.7% at baseline to 12.8% at 5 weeks. To accurately analyze cell cycle stage, we costained with Ki67 and cyclin A (Fig. 1A), revealing a significantly higher proportion of cycling cells in S or G2 phases of the cell cycle by the end of week 1 of radiotherapy (48%) as compared with baseline (29%), and the increase

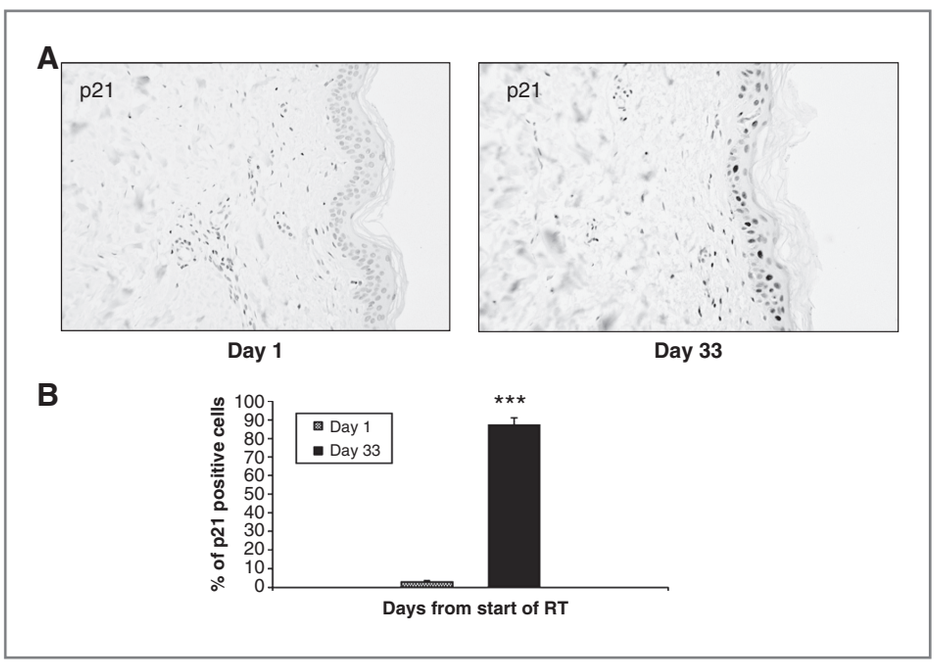

Figure 2. p21 expression in human epidermis. A, p21 staining (black nuclei) of human epidermis with haematoxylin counterstain (20×). At the start of radiotherapy there was virtually no uptake of p21 staining. However, by the 25th fraction of radiotherapy there was a dramatic increase throughout the epidermal layers. B, p21 index scored in 10 patients. Only 2.8% of cells showed mild staining 2 hours after the first fraction of radiotherapy. However, the p21 index rose dramatically to 87.4% (any positivity) at day 33 of radiotherapy ($P < 0.00002$). Error bars show *SEM*. RT, radiotherapy.

was maintained at the end of 5 weeks [$P < 0.0003$, 95% confidence interval (CI) 47.7–50.2; Fig. 1C]. These findings are consistent with other reports of human epidermis in response to fractionated radiotherapy, detected using single staining with Ki67 and cyclin A (15).

It is well established that ionizing radiation (IR) triggers cell cycle arrest, and it was initially surprising to observe a higher proportion of cycling cells after 5 weeks of radiotherapy. One explanation is that cells accumulate in cell cycle phases with enhanced capacity to survive IR-induced damage. We immunostained for the cyclin-dependent kinase inhibitor p21, which activates several DNA damage-induced cell cycle checkpoints (19). In our study, there was virtually no expression of p21 at baseline, and only 2.8% of cells showed mild (+) staining 2 hours after the first fraction of radiotherapy (95% CI 2–3.5). The p21 index subsequently rose to 87.4% by the end of 5 weeks of radiotherapy ($P < 0.0001$, 95% CI 84.1–90.6; Fig. 2A and B). When serial sections stained for cyclin A and p21 were overlaid using MATLAB 7.9 R2009b software, the cyclin A positive nuclei overlapped with strong p21 uptake (Supplementary Fig. S1).

Ki67 and cyclin A staining was seen only in the basal or first suprabasal layer, but nuclear staining of p21 was seen dispersed in all layers of the epidermis with strongest uptake in the basal compartment. The upregulated p21 in Ki67 negative (i.e., G0) cells, coupled with a decrease in the proportion of G1 cells is likely to be related to a radiation-induced G0 block as suggested by Turesson and colleagues (15). Our data suggests that although a significantly high proportion of basal cells enter the cell cycle in response to radiation-induced cell depletion, effective cell cycle checkpoint activation prevents them from entering mitosis while radiotherapy is ongoing. Staining with the mitosis marker phospho-Histone H3 does not show an increase until after the end of a 5-week course of radiotherapy (16).

RAD51 foci in basal epidermal cells increase significantly by the end of 5 weeks radiotherapy

Next, we stained for RAD51 foci formation as a measure of active homologous recombination (17). As expected, RAD51 foci were seen only in Ki67 positive cells (Fig. 3A), consistent with homologous recombination activation in S/G2 phase cells (7–9). Ki67 positive cells arrested in

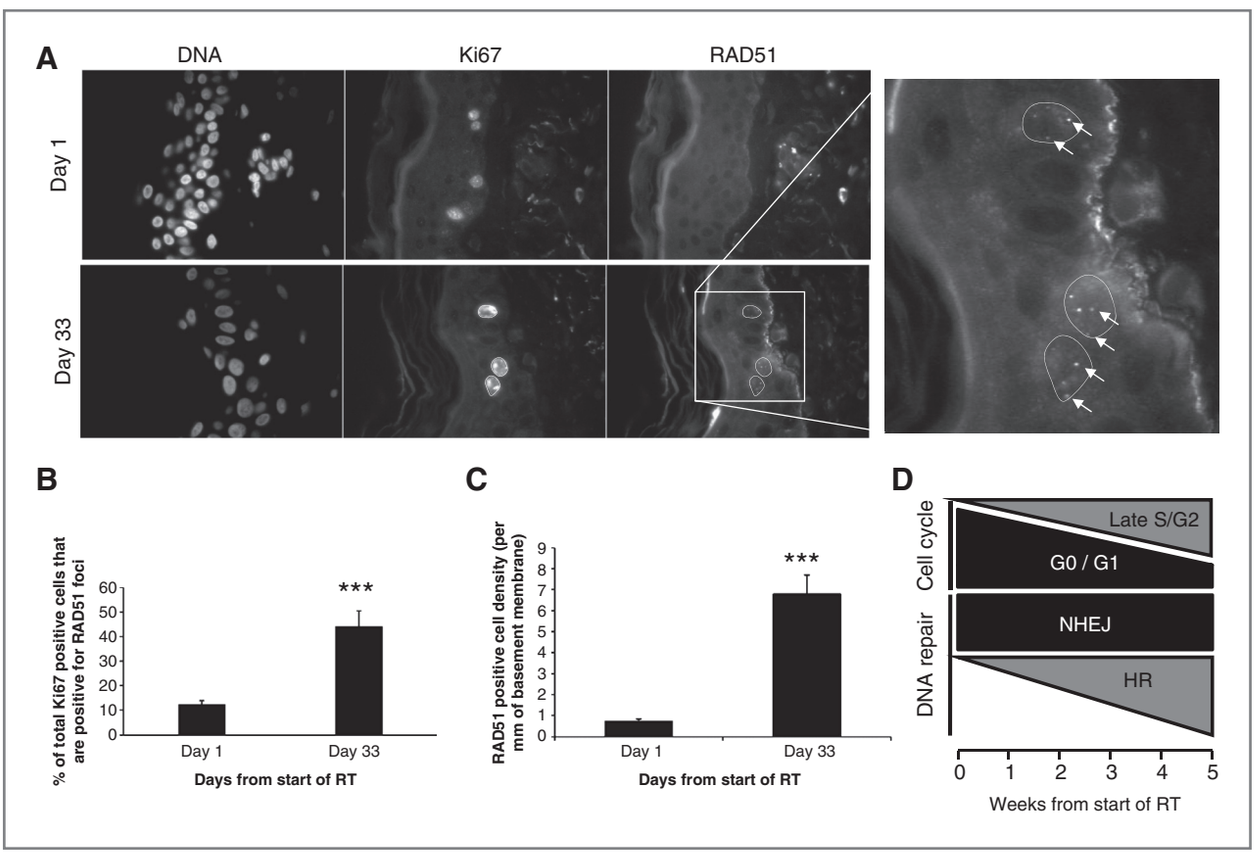

Figure 3. Changes in RAD51 expression during a course of radiotherapy. A, costaining by immmunofluorescence with Ki67, RAD51, and DAPI counterstain (100×). The top panel represents the epidermis 2 hours after the first fraction of radiotherapy where no RAD51 foci can be seen in the Ki67 positive cells. Bottom panel shows the picture 2 hours after the 25th fraction of radiotherapy and all 3 Ki67 positive cells in the field show RAD51 foci. B, between day 1 and 33, the percentage of cycling cells (Ki67 positive) containing RAD51 foci increased from 12.25% to 44.5% ($P = 0.0003$). C, RAD51 positive cell density per millimeter of basement membrane increased 9.7-fold by the end of radiotherapy. D, proposed model of changes in cell cycle and DNA DSB repair pathways with fractionated radiotherapy. Error bars represent *SEM* in 15 patients. RT, radiotherapy.

S/G2 phase are able to trigger Chk1 DNA damage response (DDR) and homologous recombination repair (20). Dual staining with Ki67 helped to identify RAD51 foci more easily as this protein is expressed only in cycling cells (21). RAD51 foci have been previously visualized in human tissue after *ex vivo* radiation (22) and *in vivo* chemotherapy (23). However, to our knowledge this is the first demonstration of RAD51 foci formation in human tissue following *in vivo* radiotherapy. The inherent background noise in tissue sections needed to be optimized to accomplish this (Fig. 3A).

The number of Ki67 positive nuclei in the basal epidermis containing RAD51 foci increased 3.9-fold between day 1 and 33 (range 2.6–7.2, $P = 0.0003$; Fig. 3B). Taking into account the increased number of Ki67 positive cells during the course of fractionated radiotherapy, the total RAD51 positive cell density (per millimeter of basement membrane) increased 9.7-fold (Fig. 3C). The mean RAD51 foci count per foci-containing cell 2 hours after the first fraction was 2.5 compared with 3.5 after the last fraction of radiotherapy ($P = 0.01$).

Cycling cells show fewer residual 53BP1 foci than noncycling cells after fractionated radiotherapy

It is well established that cells present in the late S/G2 phases are more resistant to IR as compared with other phases, pointing to homologous recombination as a possible mechanism for minimizing residual DSBs (24). To analyze DSB repair in cycling versus noncycling cells during 5 weeks of fractionated radiotherapy, we costained with Ki67 and 53BP1 (Fig. 4A). At baseline (unirradiated controls) there was no significant difference in the number of 53BP1 foci seen in Ki67 positive (mean 0.6) versus Ki67 negative cells (mean 0.7, $P = 0.1$; Fig. 4B). Interestingly, the mean number of residual foci remaining just before the last fraction of radiotherapy was 1.6 and 2.0 in Ki67 positive and negative cells, respectively ($P = 0.01$). Overall, there was a 2.6-fold ($P = 0.001$) increase in the number of residual 53BP1 foci remaining before the last fraction. However, it is not possible to say if residual foci just before the last fraction represented an accumulation of unrepaired DSB over weeks, or residual foci from the previous day's dose.

When examining 53BP1 foci 2 hours after the first fraction of radiotherapy, we found that the average foci numbers were significantly higher in Ki67 negative (5.82) versus Ki67 positive (3.48) nuclei ($P < 0.0001$; Fig. 4C). A similar finding was seen 2 hours after the last fraction with Ki67 negative cells having a mean foci number of 7.24 as compared with 4.59 in Ki67 positive cells ($P = 0.0002$; Fig. 4C). In the Ki67 positive population around 20% to 30% of nuclei failed to show distinct 53BP1 foci, but rather a diffuse

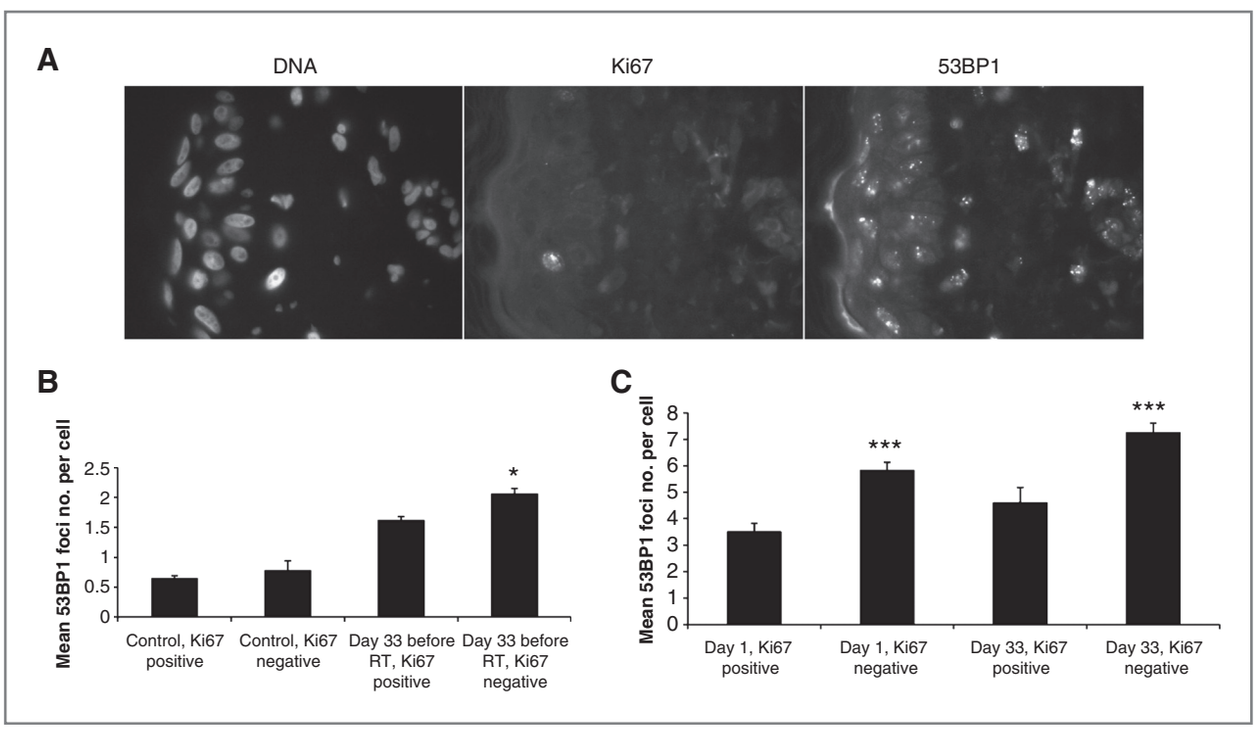

Figure 4. DNA DSB repair in proliferating versus nonproliferating cells during radiotherapy. A, double immunofluorescent staining with Ki67, 53BP1, and DAPI counterstain after the 1st fraction (100×). B, plots the mean 53BP1 foci number per cell at baseline before the 1st fraction and before the last fraction of radiotherapy in cycling versus noncycling cells. There was no significant difference in unirradiated cells, however, there were higher residual foci in noncycling cells before the last fraction ($P = 0.01$). C, shows the mean residual 53BP1 foci numbers 2 hours after the 1st and last fractions of radiotherapy in cycling versus noncycling cells. Mean foci numbers were significantly higher in Ki67 negative cells compared with Ki67 positive cells at both time points ($P < 0.0001$ day1, $P = 0.0002$ day 33). Error bars represent *SEM* in 15 patients. RT, radiotherapy.

staining pattern (similar to unirradiated nuclei) suggesting completion of DSB repair. Cells with diffuse staining pattern were scored as negative. This diffuse staining pattern was not observed in any of the Ki67 negative cells counted along the basal layer 2 hours after treatment.

The β1 integrin positive population in the basal epidermis increases during a 5-week course of radiotherapy

The human epidermis consists of quiescent stem cells and cycling progenitors/transit-amplifying cells that amplify the number of differentiated daughters resulting from each stem cell division (25). Several research groups have made extensive efforts to define a set of stem cell-specific markers in the epidermis. Much of this research has used a combination of cell adhesion molecules such as α6 or β1 integrin and the absence of cell proliferation markers such as Ki67 (25–27). In our study a combination of β1 integrin and Ki67 were used to identify putative epidermal stem cells (β1integrin ++/+++ and Ki67 negative). At baseline in unirradiated skin sections, only 20% of proliferating cells were β1 integrin positive, whereas 84% were β1 integrin positive by the end of 5 weeks of radiotherapy ($P < 0.00001$; Fig. 5). By week 5, the distinct dermal papillae had disappeared and the clustered pattern of β1 integrin staining was lost. Not only did the fraction of basal cells expressing β1 integrin increase dramatically from 5% to 10% at baseline to around 85% at week 5, the intensity of staining increased as well (Fig. 5A). Using a more specific stem cell marker MCSP (28), we found a similar change in staining pattern with radiotherapy. In the snap frozen sections, at baseline, MCSP uptake was highly clustered in a few basal cells (3%–5%), but became diffuse after 5 weeks of radiotherapy, with most of the basal layer cells staining positive (data not shown).

Discussion

Clinical data suggest that sensitivity of epidermis to fraction size varies over a 5-week course of radiotherapy, being sensitive to fraction size at the beginning of radiotherapy, and losing sensitivity during weeks 4 and 5 (10, 14). Our data suggests that activation of homologous recombination to repair DSB toward the end of radiotherapy correlates with this loss of fractionation sensitivity seen clinically. NHEJ is an error prone method of repair although homologous recombination has a high fidelity for repair that is independent of DNA damage levels (fraction size; 7). Another mechanism contributing to loss of fraction size sensitivity in S/G2 could be via cohesin, which facilitates more efficient DSB repair in replicated chromatin (29) and may enhance correct DSB repair at high doses in S/G2 in an homologous recombination-independent manner (13). The tightly bound chromatid in S/G2 might serve as a scaffold to hold break ends in place and thus avoid loss or rearrangement of chromosome material. Without such a scaffold (i.e., in G0/G1), break ends would be able to move more freely, repair would be slower and more frequently result in "wrong" ends being joined, especially at higher doses (or dose per fraction) when breaks are in close proximity. Whatever mechanisms are involved, cells in S-G2 appear to have a high fidelity for repair that is

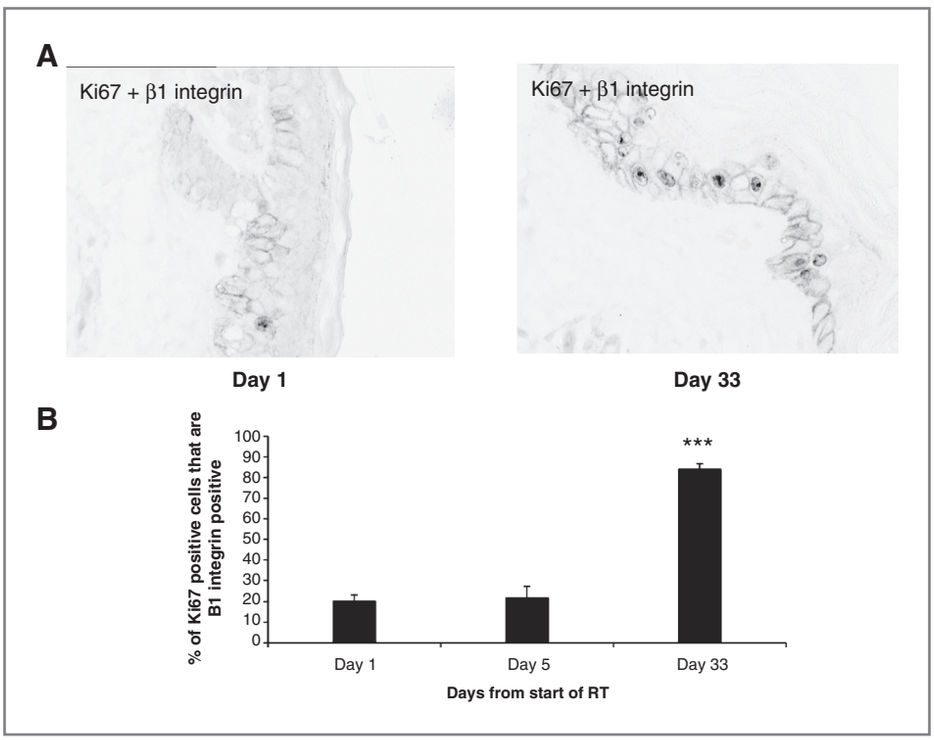

Figure 5. Changes in β1 integrin expression with radiotherapy. A, section of human breast epidermis stained immunohistochemically for the epidermal stem cell marker β1 integrin (dark gray membrane staining) and the proliferation marker Ki67 (gray/black nuclear staining) with methyl green counter stain (40×). The weak clustered pattern of β1 integrin staining at baseline changed to an intense staining by week 5 of radiotherapy with majority of basal cells being positive. There was also a significant radiotherapy-induced proliferation as quantified in Fig. 1B. B, percentage of Ki67 positive cells expressing β-1 integrin showed a significant increase from baseline to the end of 5 weeks of radiotherapy. Error bars represent *SEM* in 15 patients. RT, radiotherapy.

independent of DNA damage levels, explaining insensitivity to fraction size and mediating resistance to radiation (7, 30). Thus, a higher proportion of cells in S/G2 phase of the cell cycle (allowing greater use of high-fidelity DSB repair) is more likely to influence fractionation sensitivity than proliferation *per se* (as determined by Ki67 staining).

The 53BP1 protein accumulates in discrete nuclear foci at DSB (31), which can be used as a marker for DSB. We have been cautious in not interpreting the RAD51 and 53BP1 data in terms of relative use of homologous recombination and NHEJ for several reasons. It was technically challenging to triple stain with Ki67, RAD51, and 53BP1 and the 2-hour time point may underestimate NHEJ repair. We have therefore used 53BP1 to study the total remaining DSB and found that the number of residual DSB is lower in Ki67 positive cells as compared with Ki67 negative cells 2 hours after radiotherapy (Fig. 4C). This is surprising, as it previously has been shown that cells in G2 acquire almost twice as many DSB as those in G1 after a 2 Gy IR treatment, which is explained by the increased DNA content in G2 cells (7, 9). Thus, our finding that there are overall fewer 53BP1 foci in Ki67 positive cells suggests an increased DSB repair capacity of late S/G2 cells, probably obtained by activated homologous recombination. This is consistent with the findings of Rothkamm and colleagues in rodent cell lines (7). Residual 53BP1 foci observed before the last fraction, following 5 weeks of radiotherapy (Fig. 4B) may not just reflect unrepaired damage directly induced by radiation. It is possible that stress/senescence associated 53BP1 foci may contribute (32). Recent evidence suggests a preferential association of such foci with telomeres (33).

Supiot and colleagues have shown upregulation of p21 with a decreased Ki67 after 5 days of prostate radiotherapy suggesting that terminal growth arrest rather than apoptosis maybe the dominant mode of radiation-induced cell death in prostate epithelium (34). In our study, after the initial drop in Ki67 staining after 5 days there was a significant increase in the Ki67 staining in the basal epithelium after 5 weeks of continuous radiotherapy. This was accompanied by increased p21 staining which indicates not just G1 arrest but also G2 arrest as shown by overlaying serial sections stained for cyclin A and p21 (Supplementary Fig. S1). As shown by Turesson and coleagues, the mitosis marker phospho-Histone H3 starts to increase significantly in the basal epithelial cells after the end of radiotherapy (16). Thus, it appears that these basal epithelial cells are likely to be composed of stem/progenitor cells that have not undergone permanent cell cycle arrest/senescence. The increased p21 reflects checkpoint activation preferably in S-G2, which allows the cells to repair their DSB most efficiently. After radiotherapy these basal cells proliferate to replenish the epithelium. Our study suggests that a high proportion of cells in (or arrested in) S-G2 may influence the fractionation sensitivity of the tissue as a whole.

It is suggested that normal and cancer stem cells display a radioresistant phenotype due to activation of a DDR that enhances repair of radiation-induced DNA damage (35). The hypothesis is that stem cells make up an increasing proportion of surviving cells after each fraction of radiotherapy. In this study we found that the number of cells positive for the putative epidermal stem cell marker β1 integrin (25, 26, 27), increased during radiotherapy, in line with the notion that stem cells are radioresistant (35, 36; Fig. 5). The β1 integrin positive cells were to a high degree also Ki67 positive, suggesting that many of the stem cells have entered the cell cycle. Altogether, our data may suggest that the cells persisting after 5 weeks of radiotherapy are epidermal stem cells that have arrested in the late S-G2 phase of the cell cycle and activated homologous recombination. However, we remain very uncertain of such a conclusion as our study suggests that integrins and MCSP may not be the best markers to study stem cells in the setting of radiotherapy due to radiation-induced upregulation. Cell extracellular matrix contact mediated via integrins is thought to have an impact on cellular mechanisms resulting in increased cell survival upon exposure to IR (37, 38). Several human tumor cell lines and normal human fibroblastic cell strains have shown to increase β1 integrin expression in a dose-dependent manner following IR (39). We could not find other reports describing this in skin *in vivo*. It is difficult to comment if β1 integrin positivity after 5 weeks of radiotherapy is representative of true stemness or inherent radioresistance. However, the finding that Ki67 positive cells (the majority of which are β1 integrin positive at 5 weeks) show increased DSB repair capacity, suggest that these are surviving radiotherapy and are likely to play a role in repopulating the epidermis after radiotherapy.

Are the responses to radiotherapy in skin tissue reported here also relevant to cancer? Here, we find that epidermal cells accumulate in late S/G2 phases of the cell cycle, allowing them to trigger homologous recombination. It is widely accepted that normal fibroblast cultures with intact p53 arrest at the G1/S checkpoint, which is thought to be less leaky than the G2 checkpoint. However, there is evidence that human epidermal cells (keratinocytes) may have a differential response compared with fibroblasts, in that they predominantly arrest at the G2 checkpoint following radiation (40). The attenuated G1 arrest in keratinocytes correlated with reduced p53 accumulation compared with G1 arrested fibroblasts (40). Cancer cells often lose cell cycle checkpoints such as the p53 pathway and accumulate in the G2 phase of the cell cycle after DNA damage (41). Thus, it is highly likely that the increase in homologous recombination reported here in skin epithelial cells also extends to many cancer cells, especially those with a high-proliferative index.

In conclusion, although it is known that most of the IR-induced DSB are repaired by NHEJ in mammalian cells, our results suggest that homologous recombination plays an important role in DSB repair in the human epidermis by the end of a 5-week course of fractionated radiotherapy as cells accumulate in S/G2 phase of the cell cycle (Fig. 3D). Adoption of homologous recombination, because of its high fidelity, offers a mechanism explaining loss of fractionation sensitivity in rapidly

cycling normal and malignant tissues, and suggests a potential approach to individualization of radiotherapy dose prescription.

Disclosure of Potential Conflicts of Interest

No potential conflicts of interest were disclosed.

Authors' Contributions

Conception and design: N. Somaiah, J.R. Yarnold, K. Rothkamm, T. Helleday

Development of methodology: N. Somaiah, J.R. Yarnold, F. Daley, A. Pearson, K. Rothkamm

Acquisition of data (provided animals, acquired and managed patients, provided facilities, etc.): N. Somaiah, A. Pearson, L. Gothard, K. Rothkamm

Analysis and interpretation of data (e.g., statistical analysis, biostatistics, computational analysis): N. Somaiah, K. Rothkamm, T. Helleday

Writing, review, and/or revision of the manuscript: N. Somaiah, J.R. Yarnold, K. Rothkamm, T. Helleday

Administrative, technical, or material support (i.e., reporting or organizing data, constructing databases): N. Somaiah, F. Daley, A. Pearson, L. Gothard, T. Helleday

Study supervision: K. Rothkamm, T. Helleday

Grant Support

This study has been kindly funded by the Breast Cancer Campaign charity, grant reference 2006NovPR11, the Swedish Cancer Society and the Swedish Research Council. We also acknowledge NHS funding to the NIHR Biomedical Research Centre and the NIHR Centre for Research in Health Protection.

The costs of publication of this article were defrayed in part by the payment of page charges. This article must therefore be hereby marked *advertisement* in accordance with 18 U.S.C. Section 1734 solely to indicate this fact.

Received December 15, 2010; revised June 17, 2012; accepted July 10, 2012; published OnlineFirst August 1, 2012.

References

1. Turesson I, Nyman J, Holmberg E, Oden A. Prognostic factors for acute and late skin reactions in radiotherapy patients. Int J Radiat Oncol Biol Phys 1996;36:1065–75.
2. Thames HD, Bentzen SM, Turesson I, Overgaard M, van den Bogaert W. Fractionation parameters for human tissues and tumors. Int J Radiat Biol 1989;56:701–10.
3. Owen JR, Ashton A, Bliss JM, Homewood J, Harper C, Hanson J, et al. Effect of radiotherapy fraction size on tumour control in patients with early-stage breast cancer after local tumour excision: long-term results of a randomised trial. Lancet Oncol 2006;7:467–71.
4. Bentzen SM, Agrawal RK, Aird EG, Barrett JM, Barrett-Lee PJ, Bliss JM, et al. The UK Standardisation of Breast Radiotherapy (START) Trial A of radiotherapy hypofractionation for treatment of early breast cancer: a randomised trial. Lancet Oncol 2008;9:331–41.
5. Whelan TJ, Pignol JP, Levine MN, Julian JA, Mackenzie R, Parpia S, et al. Long-term results of hypofractionated radiation therapy for breast cancer. N Engl J Med 2010;362:513–20.
6. Steel GG. The ESTRO Breur lecture. Cellular sensitivity to low dose-rate irradiation focuses the problem of tumour radioresistance. Radiother Oncol 1991;20:71–83.
7. Rothkamm K, Kruger I, Thompson LH, Lobrich M. Pathways of DNA double-strand break repair during the mammalian cell cycle. Mol Cell Biol 2003;23:5706–15.
8. Saleh-Gohari N, Helleday T. Conservative homologous recombination preferentially repairs DNA double-strand breaks in the S phase of the cell cycle in human cells. Nucleic Acids Res 2004;32:3683–8.
9. Beucher A, Birraux J, Tchouandong L, Barton O, Shibata A, Conrad S, et al. ATM and Artemis promote homologous recombination of radiation-induced DNA double-strand breaks in G2. EMBO J 2009;28:3413–27.
10. Hopewell JW, Nyman J, Turesson I. Time factor for acute tissue reactions following fractionated irradiation: a balance between repopulation and enhanced radiosensitivity. Int J Radiat Biol 2003;79:513–24.
11. Thacker J, Wilkinson RE. The genetic basis of cellular recovery from radiation damage: response of the radiosensitive irs lines to low-dose-rate irradiation. Radiat Res 1995;144:294–300.
12. Rothkamm K, Kuhne M, Jeggo PA, Lobrich M. Radiation-induced genomic rearrangements formed by nonhomologous end-joining of DNA double-strand breaks. Cancer Res 2001;61:3886–93.
13. Kruger I, Rothkamm K, Lobrich M. Enhanced fidelity for rejoining radiation-induced DNA double-strand breaks in the G2 phase of Chinese hamster ovary cells. Nucleic Acids Res 2004;32:2677–84.
14. Turesson I, Thames HD. Repair capacity and kinetics of human skin during fractionated radiotherapy: erythema, desquamation, and telangiectasia after 3 and 5 year's follow-up. Radiother Oncol 1989;15:169–88.
15. Turesson I, Bernefors R, Book M, Flogegard M, Hermansson I, Johansson KA, et al. Normal tissue response to low doses of radiotherapy assessed by molecular markers–a study of skin in patients treated for prostate cancer. Acta Oncol 2001;40:941–51.
16. Turesson I, Nyman J, Qvarnstrom F, Simonsson M, Book M, Hermansson I, et al. A low-dose hypersensitive keratinocyte loss in response to fractionated radiotherapy is associated with growth arrest and apoptosis. Radiother Oncol 2010;94:90–101.
17. Thompson LH, Schild D. Homologous recombinational repair of DNA ensures mammalian chromosome stability. Mutat Res 2001;477:131–53.
18. Hoskin PJ, Sibtain A, Daley FM, Saunders MI, Wilson GD. The immunohistochemical assessment of hypoxia, vascularity and proliferation in bladder carcinoma. Radiother Oncol 2004;72:159–68.
19. Abbas T, Dutta A. p21 in cancer: intricate networks and multiple activities. Nat Rev Cancer 2009;9:400–14.
20. Jazayeri A, Falck J, Lukas C, Bartek J, Smith GC, Lukas J, et al. ATM- and cell cycle-dependent regulation of ATR in response to DNA double-strand breaks. Nat Cell Biol 2006;8:37–45.
21. Yamamoto A, Taki T, Yagi H, Habu T, Yoshida K, Yoshimura Y, et al. Cell cycle-dependent expression of the mouse Rad51 gene in proliferating cells. Mol Gen Genet 1996;251:1–12.
22. Willers H, Taghian AG, Luo CM, Treszezamsky A, Sgroi DC, Powell SN. Utility of DNA repair protein foci for the detection of putative BRCA1 pathway defects in breast cancer biopsies. Mol Cancer Res 2009;7:1304–9.
23. Graeser M, McCarthy A, Lord CJ, Savage K, Hills M, Salter J, et al. A marker of homologous recombination predicts pathologic complete response to neoadjuvant chemotherapy in primary breast cancer. Clin Cancer Res 2010;16:6159–68.
24. Wilson PF, Hinz JM, Urbin SS, Nham PB, Thompson LH. Influence of homologous recombinational repair on cell survival and chromosomal aberration induction during the cell cycle in gamma-irradiated CHO cells. DNA Repair (Amst) 2010;9:737–44.
25. Ambler CA, Maatta A. Epidermal stem cells: location, potential and contribution to cancer. J Pathol 2009;217:206–16.
26. Li A, Simmons PJ, Kaur P. Identification and isolation of candidate human keratinocyte stem cells based on cell surface phenotype. Proc Natl Acad Sci U S A 1998;95:3902–7.
27. Jensen UB, Lowell S, Watt FM. The spatial relationship between stem cells and their progeny in the basal layer of human epidermis: a new view based on whole-mount labelling and lineage analysis. Development 1999;126:2409–18.
28. Legg J, Jensen UB, Broad S, Leigh I, Watt FM. Role of melanoma chondroitin sulphate proteoglycan in patterning stem cells in human interfollicular epidermis. Development 2003;130:6049–63.
29. Bauerschmidt C, Arrichiello C, Burdak-Rothkamm S, Woodcock M, Hill MA, Stevens DL, et al. Cohesin promotes the repair of ionizing radiation-induced DNA double-strand breaks in replicated chromatin. Nucleic Acids Res 2010;38:477–87.
30. Utsumi H, Elkind MM. Requirement for repair of DNA double-strand breaks by homologous recombination in split-dose recovery. Radiat Res 2001;155:680–6.

31. Schultz LB, Chehab NH, Malikzay A, Halazonetis TD. p53 binding protein 1 (53BP1) is an early participant in the cellular response to DNA double-strand breaks. J Cell Biol 2000;151:1381–90.
32. Rodier F, Coppe JP, Patil CK, Hoeijmakers WA, Munoz DP, Raza SR, et al. Persistent DNA damage signalling triggers senescence-associated inflammatory cytokine secretion. Nat Cell Biol 2009;11: 973–9.
33. Hewitt G, Jurk D, Marques FD, Correia-Melo C, Hardy T, Gackowska A, et al. Telomeres are favoured targets of a persistent DNA damage response in ageing and stress-induced senescence. Nat Commun 2012;3:708.
34. Supiot S, Shubbar S, Fleshner N, Warde P, Hersey K, Wallace K, et al. A phase I trial of pre-operative radiotherapy for prostate cancer: clinical and translational studies. Radiother Oncol 2008;88:53–60.
35. Bao S, Wu Q, McLendon RE, Hao Y, Shi Q, Hjelmeland AB, et al. Glioma stem cells promote radioresistance by preferential activation of the DNA damage response. Nature 2006;444:756–60.
36. Rachidi W, Harfourche G, Lemaitre G, Amiot F, Vaigot P, Martin MT. Sensing radiosensitivity of human epidermal stem cells. Radiother Oncol 2007;83:267–76.
37. Nam JM, Chung Y, Hsu HC, Park CC. Beta1 integrin targeting to enhance radiation therapy. Int J Radiat Biol 2009;85:923–8.
38. Cordes N, Meineke V. Integrin signalling and the cellular response to ionizing radiation. J Mol Histol 2004;35:327–37.
39. Cordes N, Meineke V. Cell adhesion-mediated radioresistance (CAM-RR). Extracellular matrix-dependent improvement of cell survival in human tumor and normal cells *in vitro*. Strahlenther Onkol 2003;179: 337–44.
40. Flatt PM, Price JO, Shaw A, Pietenpol JA. Differential cell cycle checkpoint response in normal human keratinocytes and fibroblasts. Cell Growth Differ 1998;9:535–43.
41. Kastan MB, Onyekwere O, Sidransky D, Vogelstein B, Craig RW. Participation of p53 protein in the cellular response to DNA damage. Cancer Res 1991;51:6304–11.